Electrochemical Immunoassay of Membrane P-glycoprotein by Immobilization of Cells on Gold Nanoparticles Modified on a Methoxysilyl-Terminated Butyrylchitosan Matrix†

Dan Du,‡ Huangxian Ju,*,‡ Xueji Zhang,§ Jing Chen,‡ Jie Cai,‡ and Hongyuan Chen‡

Key Laboratory of Analytical Chemistry for Life Science (Education Ministry of China), Department of Chemistry, Nanjing University, Nanjing 210093, P.R. China, and Department of Chemistry, University of South Florida, 4202 East Fowler Avenue, CHE 305, Tampa, Florida 33620-5250

Received April 21, 2005; Revised Manuscript Received June 25, 2005

ABSTRACT: A strategy to detect P-glycoprotein (P-gp) on cell membrane and quantify the cell number using electrochemical immunoassay was developed by effective surface immunoreactions and immobilization of cells on a highly hydrophilic interface, which was constructed by adsorption of colloidal gold nanoparticles on a methoxysilyl-terminated (Mos) butyrylchitosan modified glassy carbon electrode (Au-CS/GCE). Atomic force microscopy studies proved that the nanoparticles adsorbed on Mos-butyrylchitosan were efficient in preventing the cell leakage and retaining the activity of immobilized living K562/ADM leukemic cells. The incubation with P-gp monoclonal antibody and then the secondary alkaline phosphatase (AP) conjugated antibody introduced AP onto the K562/ADM cell immobilized on Au-CS/GCE. The bound AP led to an amperometric response of 1-naphthyl phosphate. Under optimal conditions the response was proportional to the logarithm of cell concentration in the range from 5.0×10^4 to 1.0×10^7 cells mL^{-1} with a detection limit of 1.0×10^4 cells mL^{-1}. The results were comparable to flow cytometric analysis of P-gp expression. This proposed method was practical, convenient, and significant in the clinic and cytobiology.

Multidrug resistance (MDR)[1] is a major limiting factor to chemotherapy of cancer. It is associated with the overexpression of several proteins, the most important being P-glycoprotein (P-gp) (*1*−*3*), which is one cellular membrane 170 kDa glycoprotein encoded by the *MDR1* gene (*4*, *5*). Failure of chemotherapy to the malignant tumor is usually characterized by the overexpression of P-gp, which is believed to act as an energy-dependent drug efflux pump that causes a decrease in cytotoxic drug accumulation (*6*, *7*). Thus, evaluation of P-gp on the cell membrane is important to advance chemotherapy of the malignant tumor. Several methods have been developed to evaluate P-gp expression, including immunofluorescence assay with specific antibodies by flow cytometry (*8*, *9*), Western blot analysis (*10*), and detection based on polymerase chain reaction (PCR) (*11*, *12*). The comparison and correlation among the clinical features of some approaches have been reported (*13*). Flow cytometric assay is proved to be very productive, but it usually is time-consuming and involves a relatively expensive apparatus. Western blot analysis is difficult to quantitate the low expression level of P-gp. PCR strategy achieves more sensitive detection of MDR parameters than protein-based approaches; however, this strategy cannot exclude the possible contamination of the probe, which results in false positive signals especially in patient samples with a low blast count (*12*). In view of the above challenges, this work attempts to develop a simple and sensitive method for detection of P-gp on the tumor cell surface by combining the high selectivity of immunoassay, the good stability of immobilized living cells resulting from nanoparticles, and the high sensitivity and simplicity of electrochemical detection.

Electrochemical enzyme-linked immunoassay is a promising technique in clinical and biochemical analyses by enzymatic amplification of the signals (*14*−*17*). Alkaline phosphatase (AP) is a stable enzyme with high specific activity toward the hydrolysis of phosphate ester, such as 1-naphthyl phosphate (1-NP), which has been used to produce electroactive phenol on the immunosensor surface (*18*). Here AP was introduced onto the cell membrane by two-step immunoreactions based on effective immobilization of the cells on a glass carbon electrode (GCE) modified with colloidal gold nanoparticles and methoxysilyl-terminated

† Supported by the Distinguished Young Scholar Fund to H.J. (20325518), the National Natural Science Foundation of China (20275017, 90206037), the Science Foundation of Jiangsu (BS2001063), and the Key Project of Cancer Institute of Jiangsu Province.

* To whom correspondence should be addressed. E-mail: hxju@nju.edu.cn. Phone: (86) 25-83593593. Fax: (86) 25-83593593.

‡ Nanjing University.

§ University of South Florida.

[1] Abbreviations: MDR, multidrug resistance; P-gp, P-glycoprotein; PCR, polymerase chain reaction; AP, alkaline phosphatase; 1-NP, 1-naphthyl phosphate; GCE, glass carbon electrode; P-gp MAb, P-gp mouse monoclonal antibody; PBS, phosphate-buffered saline; FCS, fetal calf serum; CS/GCE, cross-linked Mos-butyrylchitosan modified GCE; Au-CS/GCE, colloidal gold nanoparticles assembled CS/GCE; K562/ADM-Au-CS/GCE, K562/ADM cells adhered Au-CS/GCE; AP-P-gp-K562/ADM-Au-CS/GCE, AP bound K562/ADM-Au-CS/GCE by two-step surface immunoreactions; AFM, atomic force microscopy; DPV, differential pulse voltammetric.

10.1021/bi0507332 CCC: $30.25
Published on Web 08/04/2005

Scheme 1: Mechanism for Determination of P-glycoprotein on K562/ADM Cell Surface by Electrochemical Enzyme-Linked Immunoassay

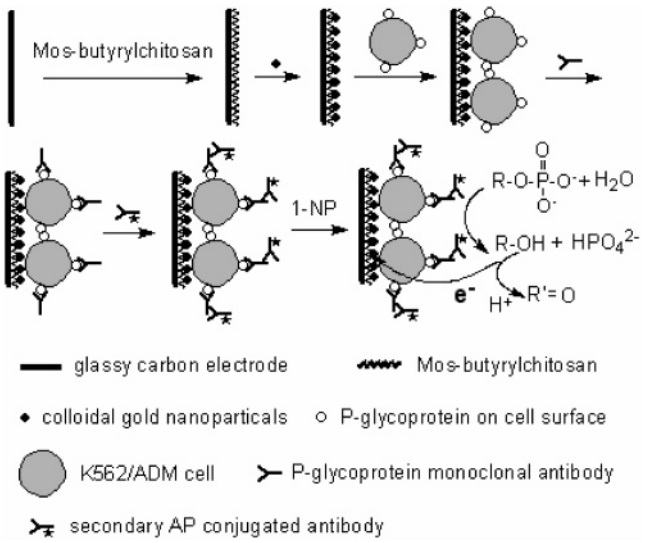

butyrylchitosan (Mos-butyrylchitosan). The immunoassay procedure was shown in Scheme 1. Chitosan, possessing various desirable properties, e.g., low cost, low toxicity, chemical inertness, high hydrophilicity, and good biocompatibility, is attractive for the immobilization of biomolecules (*19*). The functional gold nanoparticle-based material has recently emerged as a novel approach for biosensing because of its unique mechanical, electronic, and catalytic properties (*20*). In this work, the assembled colloidal gold nanoparticles on cross-linked Mos-butyrylchitosan modified GCE provide one excellent interface with good biocompatibility and analytical performance for K562/ADM cell adhesion and electrochemical immunoassay of protein expression on the cell membrane. K562/ADM cells are established from K562 human leukemia cells after they are cultured in a culture medium containing adriamycin and show typical MDR phenotype, i.e., multiple copies of MDR1 and a high level of P-gp on the cell membrane (*21*). In comparison with the results obtained from flow cytometric assay, this proposed method shows an acceptable accuracy and provides a new strategy to evaluate P-gp expression on K562/ADM cell membrane and quantify the cell number. This simple and sensitive method presents a significant tool to evaluate acceptor expression on the cell membrane and advance clinic diagnosis of MDR in the aim of successful chemotherapy of human cancers.

EXPERIMENTAL PROCEDURES

Materials. P-gp mouse monoclonal antibody (P-gp MAb, 200 μg mL^{-1}) was purchased from NeoMarkers (Fremont, CA), and the secondary antibody of AP-labeled goat anti-mouse (0.1 mg) was obtained from Kirkegaard & Perry Laboratories. Fluorescein-conjugated P-gp MAb and fluorescein-conjugated goat anti-mouse immunoglobulins were from Becton Dickinson. 1-NP was the product of Acros. Phosphate-buffered saline (PBS) (pH 7.4) containing 137 mM NaCl, 2.7 mM KCl, 87.2 mM $Na_2HPO_4 \cdot 12H_2O$, and 14.1 mM KH_2PO_4 was used as the electrolyte in the measuring system. Mos-butyrylchitosan, prepared as described in ref *22*, was the generous gift from another laboratory of Nanjing University. Colloidal gold nanoparticles (24 $\pm$ 2.1 nm diameter) were prepared and characterized with transmission electron microscopy as described before (*20*). All solutions were made with deionized water of 18 MΩ purified from a Milli-Q purification system.

Cell Lines and Culture. K562/ADM and K562 cells were kindly provided by the Affiliated Zhongda Hospital, Southeast University, Nanjing, China. K562 cells were cultured in a flask in RPMI 1640 medium (GIBCO) supplemented with 10% fetal calf serum (FCS, Sigma), penicillin (100 μg mL^{-1}), and streptomycin (100 μg mL^{-1}) at 37 °C in a humidified atmosphere containing 5% CO_2. The K562/ADM cells were maintained with 5 μg mL^{-1} adriamycin (Sigma). After 72 h the cells were collected and separated from the medium by centrifugation at 1000*g* for 10 min and then washed twice with sterile pH 7.4 PBS. The sediment was resuspended in PBS to obtain a homogeneous cell suspension with the final concentration of 2.0 $\times$ 10^6 cells mL^{-1}. Cell number was determined using a Petroff-Hausser cell counter.

Electrode Preparation and Cell Immobilization. The GCE was polished to a mirror using 0.3 and 0.05 μm alumina slurry (Beuhler) followed by rinsing thoroughly with doubly distilled water, pretreated electrochemically by applying a potential of +1.75 V in 0.1 M pH 5.0 PBS for 300 s, and scanned between +0.3 and +1.25 V and then +0.3 and −1.3 V until a steady-state current−voltage curve was observed (*23*). This process led to the formation of hydroxyl groups on the GCE surface and increased surface hydrophilicity of the GCE.

The hydrolysis of 1.0 wt % Mos-butyrylchitosan solution was performed in 0.05 M acetic acid. Then the 5 μL mixture was dropped onto a pretreated GCE to form a cross-linked Mos-butyrylchitosan modified GCE (CS/GCE) by the interaction between Mos-butyrylchitosan and the hydroxyl groups on the GCE surface, as shown in Scheme 2. After being rinsed with doubly distilled water to remove excessive uncrossed molecules, the CS/GCE was then immersed into colloidal gold solution for 30 min to prepare colloidal gold nanoparticle assembled CS/GCE (Au-CS/GCE). Following a rinse with doubly distilled water, the immobilization of cells was accomplished by dropping 5 μL of a 2.0 $\times$ 10^6 cell mL^{-1} suspension on the Au-CS surface. The obtained K562/ADM cells adhering Au-CS/GCE (K562/ADM-Au-CS/GCE) were used for subsequent immunoassay.

Electrochemical Immunoassay. The K562/ADM-Au-CS/GCE was first incubated with 5 μg mL^{-1} P-gp MAb and then with 2 μg mL^{-1} secondary AP conjugated antibody at 35 °C for 60 min, respectively. The electrochemical signal of the obtained AP-bound K562/ADM-Au-CS/GCE by two-step surface immunoreactions (AP-P-gp-K562/ADM-Au-CS/GCE) was recorded in 1.0 mL of pH 7.4 PBS containing 0.25 mM 1-NP, an optimal concentration selected at a cell concentration of 2.0 $\times$ 10^6 cells mL^{-1}, on a CHI 730 electrochemical analyzer with a conventional three-electrode system comprising platinum wire as the auxiliary, saturated calomel electrode as reference and AP-P-gp-K562/ADM-Au-CS/GCE as working electrodes.

Characterizations. Atomic force microscopy (AFM) experiments were performed on SPA-300 HV with a SPI 3800 controller (Seiko). They were carried out in liquid (PBS solution) using the tapping mode. The SI-DF-3 cantilevers (Seiko Instruments Inc.) were used (spring constant was

Scheme 2: Mechanism for Preparation of Mos-butyrylchitosan Cross-Linked on GCE

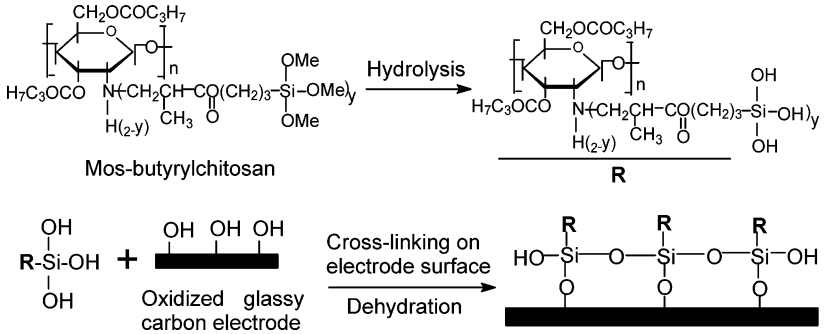

about 3 N/m, resonance frequency ranging from 90 to 150 kHz). UV spectra were recorded using a UV-2201 spectrophotometer (Shimadzu, Kyoto, Japan). The static water contact angle was measured at 25 °C by a contact angle meter (Rame-Hart-100) employing drops of pure deionized water. The readings were stabilized and taken in 120 s after dropping.

Detection of P-gp by Immunofluorescence on Flow Cytometry. Sample cells were incubated with 5 μL of 50 μg mL^{-1} fluorescein-conjugated P-gp MAb, and the control cells were incubated with the same concentration of fluorescein-conjugated goat anti-mouse immunoglobulins at 4 °C for 30 min, respectively. After being washed twice with ice-cold pH 7.4 PBS containing 10% FCS, cells were immediately analyzed on a flow cytometer (Becton Dickinson).

RESULTS

Cyclic Voltammetric Characteristics. The cyclic voltammograms of GCE, CS/GCE, Au-CS/GCE, K562/ADM-Au-CS/GCE, and AP-P-gp-K562/ADM-Au-CS/GCE did not show detectable amperometric signals in pH 7.4 PBS (Figure 1). The presence of colloidal gold nanoparticles resulted in an excessive decrease in the background current due to the decrease of the surface charge of the Au-CS film, which resulted from the interaction between the negatively charged nanoparticles and the protonated amine residue ($-NH_3^+$) in cross-linked Mos-butyrylchitosan film. However, the background current of K562/ADM-Au-CS/GCE increased greatly owing to the native system of living cells and a relatively rough surface. No peak was observed at K562/ADM-Au-CS/GCE in pH 7.4 PBS containing 0.25 mM 1-NP that could not be directly oxidized in the potential window studied. After incubation with P-gp MAb and then the secondary AP-conjugated antibody, the AP-P-gp-K562/ADM-Au-CS/GCE obtained showed an oxidation peak at +419 mV in PBS containing 1-NP. This peak came from an electron-transfer reaction of 1-naphthol. 1-Naphthol was formed from the hydrolysis of 1-NP, which was catalyzed by the conjugated AP on the electrode surface without a separate control. The principle was shown in Scheme 1. The amperometric signal was directly related to the expression of P-gp on the cell membrane, producing a method for evaluation of P-gp expression. However, after the same procedures were performed at the GCE without the presence of CS or colloids, no amperometric signal was detectable, indicating the need of the biocompatible and hydrophilic Au-CS matrix for cell adhesion. With increasing scan rate the peak current increased and was proportional to the square root of the scan rate in the range of 5−200 mV s^{-1}; thus the enzymatic reaction rate of 1-NP hydrolysis was faster than both the electron transfer of the formed 1-naphthol and the diffusion of 1-NP to the electrode surface.

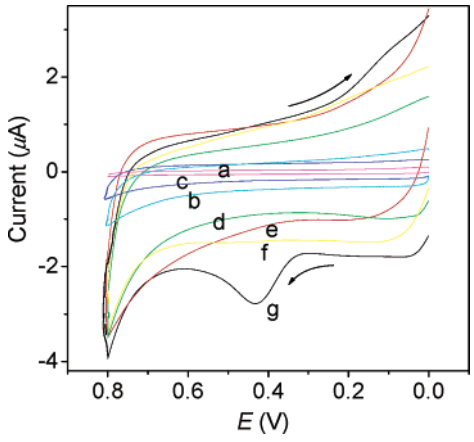

FIGURE 1: Cyclic voltammograms of (a) GCE, (b) CS/GCE, (c) Au-CS/GCE, (d) K562/ADM-Au-CS/GCE, and (e) AP-P-gp-K562/ADM-Au-CS/GCE electrodes in the absence or (f) K562/ADM-Au-CS/GCE and (g) AP-P-gp-K562/ADM-Au-CS/GCE in the presence of 0.25 mM 1-NP in pH 7.4 PBS at 50 mV s^{-1}.

Characterization of Atomic Force Microscopy. AFM measurement is an effective method to provide surface topography and phase images. As seen from Figure 2, the cross-linked Mos-butyrylchitosan film shows more uniform distribution when comparing the AFM image of the unmodified GCE (see Figure S1 in Supporting Information) with that of the chitosan film modified GCE. The height was less than 3 nm (Figure 2A). When the chitosan film was exposed to colloidal gold nanoparticles, the assembly of gold nanoparticles on the film to form a densely packed Au-CS film with a height of 10 nm could be clearly seen (Figure 2B). Upon dropping of the K562/ADM cell suspension on the obtained Au-CS film, some intact and plump cells were adhered uniformly on the film through weak interaction between colloidal gold nanoparticles and mercapto or primary amine groups on the cell membrane (Figure 2C). The adhered cells could retain their plumpness on the nanoparticle-assembled film for 2 days. The colloidal gold nanoparticles provided an environment similar to that of biomolecules in a native system and efficiently prevented cells from leakage.

Characterization of UV Spectroscopy. The binding of colloidal gold nanoparticles on cross-linked Mos-buryryl-chitosan film was characterized through UV spectroscopy at different exposure time intervals (Figure 2D). The freshly prepared colloidal gold solution showed a maximum absor-

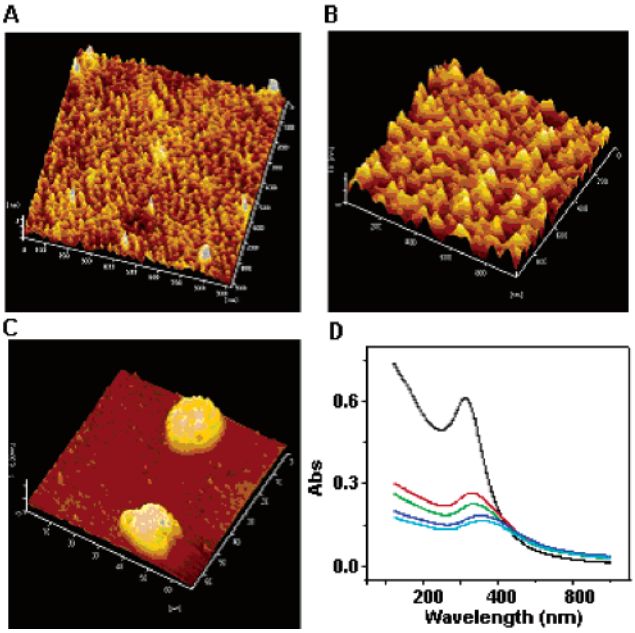

FIGURE 2: AFM images of (A) Mos-butyrylchitosan film, (B) Au-chitosan film, and (C) K562/ADM-Au-chitosan film and (D) UV spectra of different colloidal gold nanoparticle solutions obtained after immersing CS/GCE for 0 (black), 10 (red), 20 (green), 30 (blue), and 40 (cyan) min.

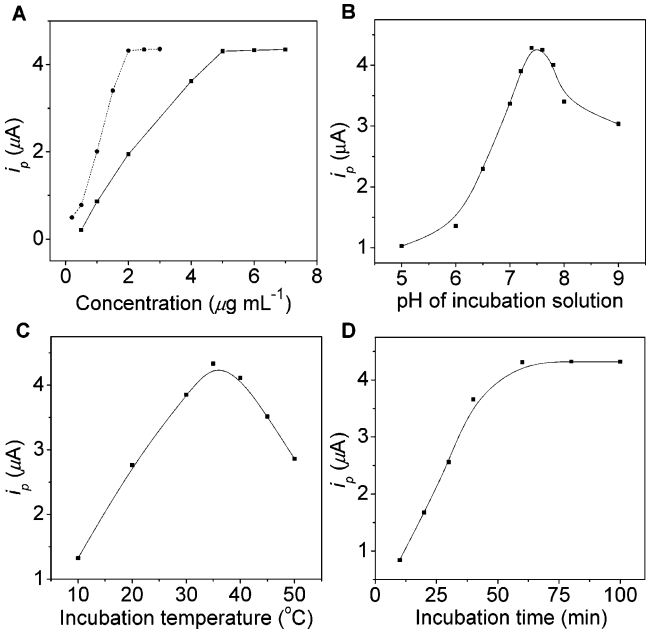

FIGURE 3: Effects of (A) concentrations of P-gp MAb (solid line) and secondary AP conjugated antibody (dash line), (B) pH of incubation solution, (C) incubation temperature, and (D) incubation time on the DPV peak. When one condition is changed, other conditions are pH 7.4, 5 μg mL^{-1} P-gp MAb, 2 μg mL^{-1} secondary AP conjugated antibody, 35 °C, and 60 min.

bance (λ_{max}) at 519 nm, which was the characteristic absorbance of unaggregated colloidal gold nanoparticles (*24*). After the CS/GCE was immersed in the solution for 10 min, the absorbance showed a great decrease, indicating the decrease of the amount of colloidal gold nanoparticles in the solution due to adsorption of some colloidal gold nanoparticles on the CS/GCE, while no obvious change of the absorbance was observed when a pretreated GCE without the chitosan layer was immersed in the solution for 10 min. The λ_{max} shifted slightly to 525 nm, which probably resulted from the aggregation of some nanoparticles in solution. With an increase of the immersing time the λ_{max} red shifted and the absorbance further decreased and then tended to a constant value, indicating a saturated adsorption of gold nanoparticles on the CS film by the strong electrostatic interaction between protonated amino groups in the Mos-butyrylchitosan polymer and gold nanoparticles. The further red shift of λ_{max} was due to the irreversible aggregation of colloidal gold nanoparticles, which resulted from the presence of the charged CS film on the electrode and the instability of the colloidal solution. Thus, the immersion time of 30 min was selected for preparation of Au-CS/GCE.

Surface Hydrophilicity. The hydrophilicity of the films was characterized by measuring the contact angle of untreated GCE and treated GCE, CS/GCE, and Au-CS/GCE. Their contact angles were 76.5°, 68.5°, 47.2°, and 40.5°, respectively. The Au-CS/GCE showed the lowest contact angle, indicating the best hydrophilic surface for cell adhesion, which improved the biocompatibility of the electrode surface for retaining cell activity (*25*).

Optimization of Immunoreaction Conditions. The amount of AP bound on K562/ADM-Au-CS/GCE was an important parameter for sensitive and reproducible immunoassay of P-gp on the cell membrane. With the increasing concentration of P-gp MAb or secondary AP conjugated antibody in the incubation solutions, both of the differential pulse voltammetric (DPV) peak currents of the obtained AP-P-gp-K562/ADM-Au-CS/GCE in PBS containing 1-NP increased linearly and then reached a constant value at the concentration of 5 μg mL^{-1} P-gp MAb or 2 μg mL^{-1} secondary AP conjugated antibody, respectively (Figure 3A), indicating that the amounts of P-gp MAb and AP conjugated antibody in the incubation solutions were enough to match the amount of P-gp molecules existing on the surface of the immobilized K562/ADM cells.

Other factors that influenced the immunoreaction included the pH of the incubation solution, the incubation temperature, and the incubation time. The optimal pH range was between 7.2 and 7.8, with the maximum response at pH 7.4 (Figure 3B), which was just the optimum pH value for living cells and usually used for the binding of enzyme-conjugated antibody with antigen. When the incubation temperature ranged from 10 to 50 °C, the maximum response occurred at 35 °C (Figure 3C). The lower response at incubation temperatures higher than 35 °C was attributed to the low activity of the enzyme due to the denaturation of bound enzyme during the incubation process. With an increasing incubation time the DPV response increased and tended to a maximum at 60 min (Figure 3D). Longer incubation time did not enhance the response. Therefore, the optimal incubation conditions were 5 μg mL^{-1} P-gp MAb and then 2 μg mL^{-1} secondary AP conjugated antibody in 1.0 mL of pH 7.4 PBS at 35 °C for 60 min.

Response to P-gp Expression and Flow Cytometric Assay. To compare the content of P-gp expressed on K562/ADM and K562 cell membrane by electrochemical enzyme-linked immunoassay, the DPV peak currents of AP-P-gp-K562/ADM-Au-CS/GCE and AP-P-gp-K562-Au-CS/GCE were determined. Under optimal immunoreaction conditions, the AP-P-gp-K562/ADM-Au-CS/GCE showed the maximum peak current of 4.32 μA at AP conjugate concentrations of

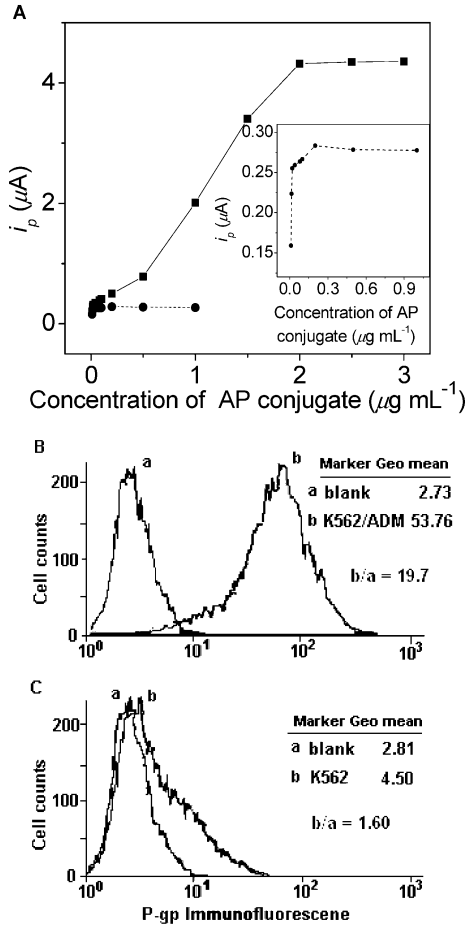

FIGURE 4: (A) Effects of concentration of AP conjugated antibody in the incubation solution on DPV peak currents of K562/ADM-Au-CS/GCE (solid line) and K562-Au-CS/GCE (dash line) in pH 7.4 PBS containing 0.25 mM 1-NP. (B, C) Flow cytometric analyses of P-gp on (B) K562/ADM cells and (C) K562 cells. Inset in (A): blowup of K562 cell plot.

more than 2 μg mL^{-1}, while the AP-P-gp-K562-Au-CS/GCE showed a maximum peak current of 0.265 μA at the AP conjugate concentration up to 0.02 μg mL^{-1} (Figure 4A). Thus the P-gp expression of K562/ADM cells was much higher than that of K562 cells. The average maximum peak current ratio of AP-P-gp-K562/ADM-Au-CS/GCE to AP-P-gp-K562−Au-CS/GCE was calculated to be 14.9 ± 1.8:1 when using 5 μL of the 5.0 × 10^6, 2.0 × 10^6, or 5.0 × 10^5 cell mL^{-1} cell suspensions to prepare the electrodes, respectively. The analyses performed on flow cytometry gave the ratio of mean fluorescent intensity of 19.7 on K562/ADM cells (Figure 4B) and 1.60 on K562 cells (Figure 4C). The ratio of K562/ADM cells and K562 cells was about 12.3:1. Obviously, the results obtained with the proposed electrochemical enzyme-linked immunoassay were acceptable.

Electrochemical Method for Cell Quantification. With an increasing concentration of K562/ADM cells for their immobilization, the DPV peak current of the 1-naphthol formed increased (Figure 5). The peak current was proportional to the logarithmic value of the cell concentration ranging from 5.0 × 10^4 to 1.0 × 10^7 cells mL^{-1} with a correlation coefficient of 0.9965. When the cell concentration for immobilization was larger than 1.0 × 10^7 cells mL^{-1}, the peak current tended to a maximum value, indicating a saturated coverage. When dropping 5 μL of the 2.0 × 10^6

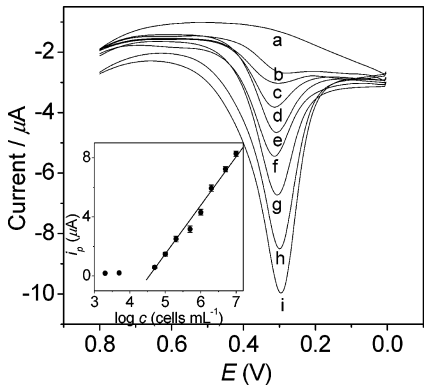

FIGURE 5: DPV curves of 0.25 mM 1-NP in pH 7.4 PBS at AP-P-gp-K562/ADM-Au-CS/GCEs prepared with different cell concentrations of (a) 0, (b) 5.0 × 10^4, (c) 1.0 × 10^5, (d) 2.0 × 10^5, (e) 5.0 × 10^5, (f) 1.0 × 10^6, (g) 2.0 × 10^6, (h) 5.0 × 10^6, and (i) 1.0 × 10^7 cells mL^{-1}. Inset: plot of DPV peak current vs logarithm of cell concentration.

cell mL^{-1} suspension on the Au-CS surface, the coverage of cells on the surface was obtained from an inverse microscopic image (see Figure S2, Supporting Information) to be 7.2 × 10^4 cells cm^{-2}, which was 95% of saturated coverage of the film. The detection limit for cell number was calculated to be 1.0 × 10^4 cells mL^{-1} at 3σ, which was comparable with those of several methods developed by other researchers, such as 1.0 × 10^5 cells mL^{-1} of immunomagnetic separation/flow injection analysis/mediated amperometric detection (*26*), 10^6 cells mL^{-1} of electrochemical impedance immunosensor for *Escherichia coli* O157:H7 (*27*), 1.0 × 10^4 cells mL^{-1} of immunosensor for detection of *Salmonella* species based on a quartz crystal microbalance (*28*), 6.0 × 10^3 cells mL^{-1} of immunobiosensor chip for detection of *E. coli* O157:H7 (*29*), and 7.1 × 10^2 cells mL^{-1} of immunoligand assay/light-addressable potentiometry (*30*). Thus, the presented strategy provided a simple and practical method for antibody−antigen conjugate analysis on the electrode, electrochemical immunoassay of protein expression on the cell surface, and cell quantification with high sensitivity and good accuracy.

Reproducibility and Stability of AP-P-gp-K562/ADM-Au-CS/GCE. The reproducibility of the AP-P-gp-K562/ADM-Au-CS/GCE for immunoassay was investigated with intra- and interassay precision. The intraassay precision was evaluated by assaying the peak current at one prepared electrode for five replicate measurements. The relative standard deviation of intraassay on this method was 7.5%. The interassay precision, or the fabrication reproducibility, was estimated by determining the peak current with three AP-P-gp-K562/ADM-Au-CS/GCEs made independently. The relative standard deviation of the interassay on this method was 17.8%, showing an acceptable reproducibility.

When AP-P-gp-K562/ADM-Au-CS/GCE was stored in pH 7.4 PBS at 4 °C, it retained 90% of its initial current after a 48 h storage. The AP-P-gp-K562/ADM-Au-CS/GCE, obtained by two-step surface immunoreactions after a 48 h storage of the K562/ADM-Au-CS/GCE in pH 7.4 PBS at 4 °C, also showed 90% of the current of AP-P-gp-K562/ADM-Au-CS/GCE prepared without storage. Thus 90% of the activity level of the immobilized cells remained after 2 days. This indicated that colloidal gold nanoparticles assembled on Mos-buryrylchitosan film were very efficient for retaining

the activity of living cells and preventing them from leakage away the electrode surface.

DISCUSSION

The K562/ADM leukemia cells immobilized on the electrode via the Au-chitosan matrix showed high activity for immunoreaction between P-gp expressed on K562/ADM and P-gp MAb. The immunocomplex formed could further react with the secondary AP conjugated antibody, which introduced AP onto the electrode surface for electrochemical immunoassay of P-gp expression by an enzymatic hydrolysis of 1-NP to produce the electroactive compound, 1-naphthol. The enzymatic reaction rate was very fast. Thus the produced amperometric signal was directly related to the total amount of P-gp on the cell membrane. The amperometric response increased linearly with the increasing logarithmic value of the cell concentration, producing a novel method for cell quantification. According to the fundamental of immunoassay, the level of P-gp expression on the cell membrane could be determined quantitatively if pure P-gp could be gotten to obtain one calibration or working curve. The results obtained with two kinds of cells at different concentrations showed that this method was feasible. This method is very simple and cheaper than other developed quantitative methods.

For immobilization of cells on the electrode, one biocompatible interface should first be obtained. This work formed one cross-linked Mos-butyrylchitosan film on the GCE surface for assembly of colloidal gold nanoparticles, which was well-known as a biocompatible and hydrophilic matrix for immobilization of biomolecules. When the hydrolysis mixture of 1.0 wt % Mos-butyrylchitosan was dropped onto an untreated GCE, one film could also be formed. But the film formed was unstable, so that it could be easily removed upon rinsing. Both the AFM images and the UV spectroscopic characterization indicated that the assembly of colloidal gold nanoparticles produced one hydrophilic and densely packed Au-CS film. The hydrophilicity resulted from a large number of negatively charged groups on the colloidal gold nanoparticle surface. These negatively charged groups were favorable to the assembly of colloidal gold nanoparticles due to the strong electrostatic interaction with the protonated amine residue ($-NH_3^+$) in the cross-linked Mos-butyrylchitosan film. At the same time the colloidal gold nanoparticles could adhere cells by the weak interaction between the nanoparticles and mercapto or primary amine groups on the cell membrane and provided an environment similar to the native system of living cells, thus retaining the activity of immobilized cells and proteins on the cell membrane.

The incubation conditions for the immunoassay for K562/ADM cells were pH 7.4 PBS at 35 °C for 60 min. An overly high incubation temperature resulted in the denaturation of the antigen, the antibody, or the bound enzyme. But a low incubation temperature decreased the rate of immunoreaction. Thus, the plot of amperometric response vs incubation temperature showed one maximum value at 35 °C. When the pH value of the incubation solution was higher or lower than pH 7.4, the immunoreaction rate between immobilized P-gp and P-gp MAb decreased, and the P-gp or P-gp MAb molecules would also denature at overly high or very low pH; thus the amperometric response of the resulting AP-P-gp-K562/ADM-Au-CS/GCE in 1-NP solution decreased. Furthermore, the pH value of the detection solution was also very important. When the pH was higher than 8.0, the response signal decreased, which was attributed to the decrease of cell activity and the weakening of interaction between the amine residue in the cross-linked Mos-butyrylchitosan film and colloidal gold nanoparticles as well as the interaction between the immobilized cells and colloidal gold nanoparticles. The low pH condition was a disadvantage to the enzymatic hydrolysis of 1-NP. Thus, pH 7.4 was an optimum pH of AP for amperometric detection.

This work combines the high selectivity of immunoreaction with high sensitivity of enzymatic amplification to develop a novel simple approach to detect glycoprotein expressed on the cell membrane. The living intact and plump cells are stably adhered on this hydrophilic and biocompatible matrix. In comparison with the results obtained by flow cytometric assay, this proposed method shows an acceptable accuracy and provides a new strategy to evaluate P-glycoprotein expression on the K562/ADM cell surface and quantify the cell number. This simple and sensitive method presents a significant field to evaluate acceptor expression on the cell membrane and advance clinic diagnosis of MDR with the aim of successful chemotherapy of human cancers.

SUPPORTING INFORMATION AVAILABLE

AFM image of the pretreated GCE (Figure S1) and the inverse microscopic image of K562/ADM leukemic cells on the Au-CS surface (Figure S2). This material is available free of charge via the Internet at http://pubs.acs.org.

REFERENCES

1. Bradley, G., Juranka, P. F., and Ling, V. (1988) Mechanisms of multidrug resistance, *Biochim. Biophys. Acta 948*, 87−128.
2. Endicott, J. A., and Ling V. (1989) The biochemistry of P-glycoprotein mediated multidrug resistance, *Annu. Rev. Biochem. 58*, 137−171.
3. Gottesman, M. M., Hrycyna, C. A., Schoenlein, P. V., Germann, U. A., and Pastan, I. (1995) Genetic analysis of the multidrug transporter, *Annu. Rev. Genet. 29*, 607−649.
4. Chen, C., Chin, J. E., Ueda, K., Clark, D. P., Pastan, I., Gottesman, M. M., and Roninson, I. B. (1986) Internal duplication and homology with bacterial transport proteins in the mdr1 (P-glycoprotein) gene from multidrug resistance human cells, *Cell 47*, 381−389.
5. Kartner, N., Riordan, J. R., and Ling, V. (1983) Cell surface P-glycoprotein associated with multidrug resistance in mammalian cell lines, *Science 221*, 1285−1288.
6. Hamada, H., and Tsuruo, T. (1986) Functional role for the 170 to 180-Kda glycoprotein specific to drug-resistant tumor cells as revealed by monoclonal antibodies, *Proc. Natl. Acad. Sci. U.S.A. 83*, 7785−7789.
7. Hamada, H., and Tsuruo, T. (1988) Characterization of the ATPase activity of the Mr 170000 to 180000 membrane glycoprotein (P-glycoprotein) associated with multidrug resistance in K562/ADM cells, *Cancer Res. 48*, 4926−4932.
8. Koizumi, S., Konishi, M., Ichihara, T., Wada, H., Matsukawa, H., Goi, K., and Mizutani, S. (1995) Flow cytometric functional analysis of multidrug resistance by fluo-3: a comparison with rhodamine-123, *Eur. J. Cancer 31A*, 1682−1688.
9. Che, X. F., Nakajimaa, Y. C., Sumizawaa, T., Ikedaa, R., Rena, X. Q., Zhenga, C. L., Mukaia, M., Furukawaa, T., Haraguchia, M., Gaoa, H., Sugimotob, Y., and Akiyamaa, S. I. (2002) Reversal of P-glycoprotein mediated multidrug resistance by a newly synthesized 1,4-benzothiazipine derivative, JTV-519, *Cancer Lett. 187*, 111−119.
10. Marks, D. C., Davey, M. W., Davey, R. A., and Kidman, A. D. (1995) Expression of multidrug resistance in response to dif-

ferentiation in the K562 human leukaemia cell line, *Biochem. Pharmacol. 50*, 475−480.
11. King, M., Su, W., Chang, A., Zuckerman, A., and Pasternak, G. W. (2001) Transport of opioids from the brain to the periphery by P-glycoprotein: peripheral actions of central drugs, *Nat. Neurol. 4*, 268−274.
12. Illmer, T., Schaich, M., Oelschlagel, U., Nowak, R., Renner, U., Ziegs, B., Subat, S., Neubauer, A., and Ehninger, G. (1999) *Leukemia Res. 23*, 653−663.
13. Maynadie, M., Matutes, E., and Catovsky, D. (1997) Quantification of P-glycoprotein in chronic lymphocytic leukemia by flow cytometry, *Leukemia Res. 21*, 825−831.
14. McNeil, C. J., Athey, D., and Ho, W. O. (1995) Direct electron-transfer bioelectronic interfaces: application to clinical analysis, *Biosens. Bioelectron. 1*, 75−83.
15. Duan, C., and Meyerhoff, M. E. (1994) Separation-free sandwich enzyme immunoassays using microporous gold electrodes and self-assembled monolayer/immobilized capture antibodies, *Anal. Chem. 66*, 1369−1377.
16. Bauer, C. G., Eremenko, A. V., Ehrentreich-Förster, E., Bier, F. F., Makower, A., Halsall, H. B., Heineman, W. R., and Scheller, F. W. (1996) Zeptomole-detecting biosensor for alkaline phosphatase in an electrochemical immunoassay for 2,4-dichlorophenoxyacetic acid, *Anal. Chem. 68*, 2453−2458.
17. Wang, J., Pamidi, P. V. A., and Rogers, K. R. (1998) Sol-Gel derived thick-film amperometric immunosensors, *Anal. Chem. 70*, 1171−1175.
18. Gehring, A. G., Brewster, J. D., Irwin, P. L., Tu, S. I., and Van Houten, L. J. (1999) 1-Naphthyl phosphate as an enzymatic substrate for enzyme-linked immunomagnetic electrochemistry, *J. Electroanal. Chem. 469*, 27−33.
19. Wang, G., Xu, J. J., Chen, H. Y., and Lu, Z. H. (2003) Amperometric hydrogen peroxide biosensor with sol−gel/chitosan network-like film as immobilization matrix, *Biosens. Bioelectron. 18*, 335−343.
20. Liu, S. Q., and Ju, H. X. (2002) Renewable reagentless hydrogen peroxide sensor based on direct electron transfer of horseradish peroxidase immobilized on colloidal gold-modified electrode, *Anal. Biochem. 307*, 110−116.
21. Kotaki, M., Motoji, T., Takanashi, M., Wang, Y. H., and Mizoguchi, H. (2003) Anti-proliferative effect of the tyrosine kinase inhibitor STI571 on the P-glycoprotein positive K562/ADM cell line, *Cancer Lett. 199*, 61−68.
22. Zhu, A. P., Wu, H., and Shen, J. (2004) Preparation and characterization of a novel Si-containing crosslinkable O-butyryl-chitosan, *Colloid Polym. Sci. 282*, 1222−1227.
23. Dai, Z., Yan, F., Chen, J., and Ju, H. X. (2003) Reagentless amperometric immunosensors based on direct electrochemistry of horseradish peroxidase for rapid determination of carcinoma antigen-125, *Anal. Chem. 75*, 5429−5434.
24. Huang, H. Z., and Yang, X. R. (2003) Chitosan mediated assembly of gold nanoparticles multiplayer, *Colloids Surf., A 226*, 77−86.
25. Kaji, H., Kanada, M., Oyamatsu, D., Matsue, T., and Nishizawa, M. (2004) Microelectrochemical approach to induce local cell adhesion and growth on substrates, *Langmuir 20*, 16−19.
26. Perez, F. G., Mascini, M., Tothill, I. E., and Turner, A. P. F. (1998) Immunomagnetic separation with mediated flow injection analysis amperometric detection of viable *Escherichia coli* O157, *Anal. Chem. 70*, 2380−2386.
27. Yang, L., Li, Y. B., and Erf, G. F. (2004) Interdigitated array microelectrode-based electrochemical impedance immunosensor for detection of *Escherichia coli* O157:H7, *Anal. Chem. 76*, 1107−1113.
28. Wong, Y. Y., Ng, S. P., Ng, M. H., Si, S. H., Yao, S. Z., and Fung, Y. S. (2002) Immunosensor for the differentiation and detection of Salmonella species based on a quartz crystal microbalance, *Biosens. Bioelectron. 17*, 676−684.
29. Ruan, C., Yang, L., and Li, Y. (2002) Immunobiosensor chips for detection of *Escherichia coli* O157:H7 using electrochemical impedance spectroscopy, *Anal. Chem. 74*, 4814−4820.
30. Gehring, A. G., Patterson, D. L., and Tu, S. (1998) Use of a light-addressable potentiometric sensor for the detection of *Escherichia coli* O157:H7, *Anal. Biochem. 258*, 293−298.

BI0507332